ICES Journal of Marine Science, 2023, **80**, 329–341
DOI: 10.1093/icesjms/fsac241
Advance access publication date: 25 January 2023
Original Article

Detection efficiency of an autonomous underwater glider carrying an integrated acoustic receiver for acoustically tagged Pacific herring

Alysha D. Cypher [1,*], Hank Statscewich [2], Robert Campbell [1], Seth L. Danielson [2], John Eiler [3] and Mary Anne Bishop [1]

[1]Prince William Sound Science Center, 1000 Orca Rd. Cordova, AK 99574, USA
[2]University of Alaska Fairbanks, College of Fisheries and Ocean Sciences, 2150 Koyukuk Drive, Fairbanks, AK 99775, USA
[3]National Marine Fisheries Service, Alaska Fisheries Science Center, Auke Bay Laboratories, 17109 Point Lena Loop Road, Juneau, AK 99801, USA

[*] *Corresponding author: tel: + 907 424 4258; fax: + 907 424 5820;* email: acypher@pwssc.org.

Autonomous underwater vehicles (AUVs) or gliders are increasingly being used with acoustic telemetry to elucidate fish movements while collecting simultaneous environmental data. We assessed the utility of an AUV equipped with an integrated acoustic receiver to detect Pacific herring (*Clupea pallasii*) in Prince William Sound, AK, USA. A range test evaluated the effect of glider flight characteristics and environmental conditions on the detection efficiency of transmitters at varying depths. While distance from transmitters was the strongest predictor of detections, glider depth had a variable effect on detection efficiency which depended on transmitter depth and dive orientation. The detection efficiency of the glider-mounted acoustic receiver was less affected by wind speed and water level than that of stationary acoustic receivers deployed within the study area. The AUV also performed repeated, adaptive transects in an area of ~630 km^2 area and detected 30 Pacific herring transmitters without *a priori* knowledge of their locations. Of these herring transmitters, 14 were presumed shed after repeated detections within the same area, and 2 were detected at multiple locations. This study is the first to demonstrate that glider-mounted acoustic receivers have high detection efficiency for transmitters at varying depths and can detect movements of migratory forage fish in large search areas.

Keywords: acoustic telemetry, autonomous underwater vehicles, detection efficiency, gliders, Pacific herring.

Introduction

Passive acoustic telemetry provides a means to study the migratory behaviour of acoustically tagged fish using automated, stationary listening stations. These listening stations, acoustic receivers or hydrophones, can repeatedly detect and identify acoustically tagged fish that pass within range of a receiver, generally <1 km depending on equipment and weather conditions (Eiler and Bishop, 2016). While there are many advantages to this methodology, there are trade-offs between the probability of detecting acoustically tagged fish and providing enough spatial receiver coverage to represent large areas used by migratory fish. Vessel-based acoustic telemetry allows users to cover a larger area than stationary receivers, but the signal strength of acoustic transmissions degrades with higher vessel engine or sea surface noise (Eiler *et al.*, 2013; Mathies *et al.*, 2014). Alternatively, autonomous underwater vehicles (AUVs) or gliders are becoming an efficient, mobile alternative for acoustic receiver mounting that offers simultaneous environmental monitoring.

AUVs can carry acoustic receivers as payload to detect acoustically tagged fish (Grothues *et al.*, 2010; Eiler *et al.*, 2013; Eiler *et al.*, 2019), evaluate fish distributions (Dodson *et al.*, 2018; Zemeckis *et al.*, 2019), characterize fish habitat (Grothues *et al.*, 2008; Haulsee *et al.*, 2015), and document the influence of oceanographic features on fish movement (Oliver *et al.*, 2013; Breece *et al.*, 2016). Glider-mounted platforms overcome some of the limitations of passive acoustic telemetry by allowing users to track individual telemetered fish and explore habitats not suitable for stationary passive receivers (Grothues *et al.*, 2008; Oliver *et al.*, 2013; Zemeckis *et al.*, 2019). In comparison to vessel-based acoustic telemetry, AUVs operate remotely and sample throughout the water column, which provides a higher detection probability in deeper waters (Eiler *et al.*, 2013). Changes in buoyancy create vertical movement, which is turned into forward propulsion by lift from the wings (Webb et al., 2001). This makes AUVs an energy-efficient option for longer deployments. While AUVs provide many advantages, they also introduce mobility to the listening platform and a broader range of environmental conditions that may affect acoustic detection efficiency. Therefore, the purpose of this work was to evaluate how glider mobility and varying environmental conditions affect acoustic detections and determine whether the glider-mounted receiver can detect acoustically tagged fish in the study area.

Due to the numerous factors that can influence detections on a mobile platform, the first objective of this study was to evaluate the detection efficiency of the AUV-mounted acoustic receiver. This was accomplished with a range test whereby the probability of detecting individual transmissions (detection efficiency) from acoustic transmitters was compared to glider flight characteristics (e.g. distance, depth, etc.) and oceano-

Received: October 14, 2022. **Revised:** December 20, 2022. **Accepted:** December 21, 2022

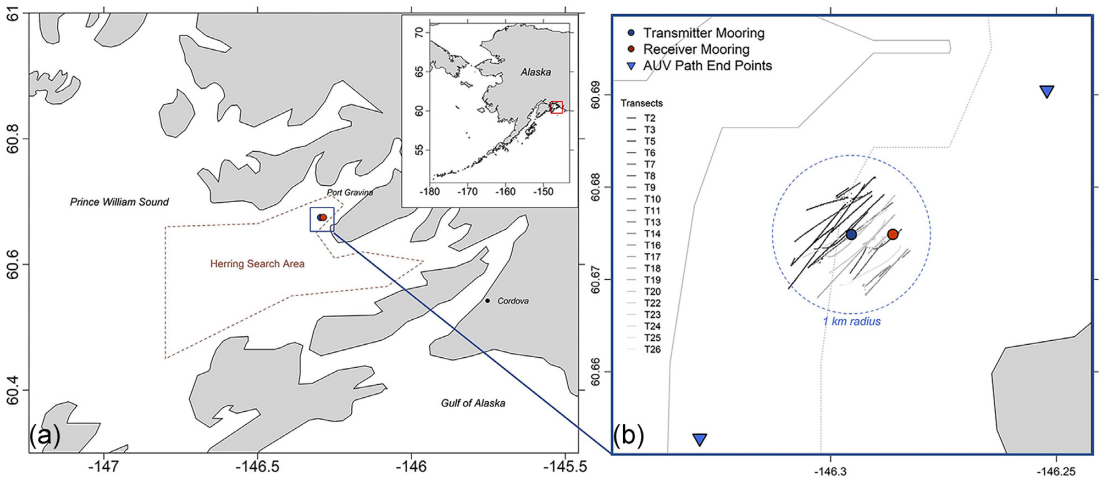

Figure 1. Map of study area within southeast PWS (a) and range test area (b) in Port Gravina. The glider conducted a range test to evaluate the detection efficiency of the glider-mounted VR2C for acoustic transmitters and repeatedly transited a 630 km^2 herring search area (a; dashed polygon) to detect acoustically tagged Pacific herring. For the range test (b), the glider conducted transects (T) between programmed AUV end points with the transmitter moored at the centre. The transmitter mooring was equipped with three acoustic transmitters at varying depths (4, 64, and 119 m) and a stationary VR2AR acoustic receiver at 124 m (TMR_124). An adjacent receiver mooring was equipped with a VR2AR at 126 m (RMR_126) and a VR2W at 65 m (RMR_65).

graphic conditions (e.g. gust speed, water level, etc.). It is evident that the detection efficiency of both stationary and mobile acoustic receivers is affected by distance from transmitters, ambient noise, and local environmental conditions (Shroyer and Logsdon, 2009; How and de Lestang, 2012; Gjelland and Hedger, 2013; Kessel *et al.*, 2014; Mathies *et al.*, 2014; Huveneers *et al.*, 2016; Klinard *et al.*, 2019). Few investigations have assessed how the mobility of the glider-mounted platform affects acoustic detection efficiency (Eiler *et al.*, 2013; Oliver *et al.*, 2017; Ennasr *et al.*, 2020). These range tests identified glider orientation in relation to transmitters (Ennasr *et al.*, 2020), water depth, and wind speed (Oliver *et al.*, 2017) as important factors that influence acoustic detections. Ocean stratification is another factor that frequently affects acoustic detections when receivers and transmitters are positioned on opposing sides of a thermocline (Shroyer and Logsdon, 2009; Cagua *et al.*, 2013; Mathies *et al.*, 2014). Here, we expanded on these range tests by including transmitters at varying depths and environmental variables relevant to subarctic oceanographic conditions.

In addition to detection efficiency, it was important to evaluate whether the glider-mounted platform could detect acoustically tagged Pacific herring (*Clupea pallasii*), an ecologically important forage fish species in our study area, Prince William Sound (PWS), AK, USA. PWS is a subarctic embayment bordering the Gulf of Alaska (GoA) in southcentral Alaska (Figurie 1a). PWS was once home to a robust Pacific herring population and fishery prior to its collapse in 1993, four years after the *Exxon Valdez* oil spill (EVOS). Since 2013, the migratory patterns of the PWS herring population have been monitored using the Ocean Tracking Network (OTN; Dalhousie University, Nova Scotia, Canada), arrays of stationary acoustic receivers across the major entrances connecting PWS to the GoA. These arrays record the date, time, and identity of acoustically tagged herring entering PWS from the GoA or exiting PWS into the GoA. Because herring are the only remaining fish species designated as injured after the EVOS (EVOS, 2014), their movements within PWS are relevant for assessing why this population has yet to recover. Therefore, our second objective was to determine whether the glider-mounted acoustic receiver could detect acoustically tagged herring in southeast PWS, an ~630 km^2 area, without *a priori* knowledge of their location.

The OTN has revealed how herring migrate out and into PWS with seasonality and that the PWS herring population consists of both resident and migratory fish (Eiler and Bishop, 2016; Bishop and Eiler, 2018; Bishop and Bernard, 2021). Due to the design of the OTN, the movement of herring within PWS is relatively unknown. Stationary acoustic receivers are not well suited for evaluating herring movements within PWS due to geography, oceanographic conditions that result in equipment loss, and the expense of receivers. While an AUV-mounted acoustic receiver provides more spatial coverage than stationary receivers, it can be difficult to track fish in large areas without *a priori* knowledge of their location. Other AUV-based acoustic telemetry studies have successfully detected telemetered fish by releasing animals within proximity to glider transects (Eiler *et al.*, 2013; White *et al.*, 2016; Eiler *et al.*, 2019; Zemeckis *et al.*, 2019), while fewer have searched large areas without recent detection data or observations (Oliver *et al.*, 2013). Repeated detections of individual herring transmitters by the glider-mounted acoustic receiver would provide novel data for the PWS study area and support the broader use of glider platforms for studying migratory fish in marine environments.

The purpose of this study was to determine whether a glider-mounted acoustic receiver would supplement the existing OTN infrastructure to study the movements of Pacific herring. The performance of the glider-mounted acoustic receiver was delineated into detection efficiency, whether it had a high probability of detecting transmitters at different depths under varying mobile and environmental conditions, and its ability to detect acoustically tagged herring in a large area without *a priori* knowledge of their location.

Table 1. Details on time and location for each glider deployment during the study period.

Deployment #	Start date	Latitude	Longitude	Duration (days)
1	25/01/2021	60.672°N	−146.767°W	29
2	23/03/2021	60.587°N	−146.010°W	29
3	29/04/2021	60.588°N	−145.974°W	28

Methods

Study area

PWS is located on the coast of southcentral Alaska, primarily between latitudes 60° and 61°N (Figure 1a). A number of marine passageways, including Hinchinbrook Entrance and Montague Strait, provide access to PWS from the northern GoA. The southeast PWS study area included Port Gravina and Orca Bay, with the range test focusing on a 1 km radius around stationary moorings in Port Gravina (Figure 1b).

Glider deployment

Between 25 January and 27 May of 2021, a Teledyne Webb Slocum AUV or glider was deployed three times in southeast PWS (Table 1). Recovery and re-deployment were required for battery recharges, recovery of full-resolution data, and maintenance. After a series of range tests and survey transects to detect acoustically tagged herring, the AUV transited into Montague Strait for 4 d and exited PWS into the GoA. Final recovery occurred in Resurrection Bay, AK, USA. The total survey distance was 1531 km over an 86-d deployment.

Prior to deployment, the AUV was equipped with an VR2C acoustic receiver (Innovasea; Bedford, Nova Scotia, Canada) that was positioned forward on the nose of the glider and programmed to detect 69 kHz acoustic transmitters for both the range test and herring search transects. The VR2C was programmed to listen for transmitters during diving, hovering, and climbing mission states and turned off when the glider was commanded to surface. The AUV was also equipped with a SeaBird conductivity, temperature, and depth (CTD) sensor, a Wet Labs Ecopuck fluorometer, a RinkoII optode for oxygen saturation measurements, and a Biospherical Instruments PAR sensor. The Wet Labs Ecopuck sensor was configured to measure optical backscatter at 700 nm and chlorophyll-*a* concentration using fluorescence. The glider estimated depth-averaged velocity between surface events by comparing surface GPS locations with dead-reckoning subsurface navigation (Schofield *et al.*, 2007).

During deployments, the glider performed surface events every 2 h by inflating an air bladder to transmit data files to a central server through an onboard iridium phone. During each surface event, the first downcast for temperature, salinity, chlorophyll-*a*, backscatter, PAR, and dissolved oxygen (subsampled every 8 s) in addition to all VR2C detections were transmitted. Before returning to its dive profile, the glider turned on a GPS receiver to obtain latitude and longitude data and downloaded new mission files. In total, surface events lasted 10 min, during which time the VR2C did not make acoustic detections.

The AUV was equipped with a magnetic drive propeller designed to prevent the glider from going off course due to strong currents. Typical horizontal glider speeds while surveying in eastern PWS were between 0.1 and 0.3 m s^{-1}. During the transit through Montague Strait, tidal currents approached 0.5 m s^{-1}, and required that the magnetic drive propellor be activated. After exiting into the GoA, the thruster was turned off until final recovery in Resurrection Bay, near Seward, AK, USA. The effect of the propeller activation on detection efficiency was not evaluated.

Range test

To evaluate the detection efficiency of the glider-mounted VR2C, a range test was conducted in southern Port Gravina (Figure 1). The glider conducted a total of 26 transects within a 1 km range of a transmitter mooring (Figure 1b) fitted with three acoustic transmitters (Model V9-2x; 146 dB power output; 4.7 g wt in air; 804 d estimated battery life; 70–150 s delay; Innovasea) at varying depths (surface, 4 m; mid-water, 65 m; near-bottom, 119 m) and a VR2AR acoustic receiver (TMR_124; Innovasea) at 124 m. Transmitter depths were chosen to represent a depth range relevant for detecting Pacific herring. During the winter months, herring schools are typically found at a lower depth (50–85 m) than in the spring, when herring concentrate near the surface to feed on zooplankton (Carlson, 1980).

A receiver mooring (Figure 1b) was also deployed, 0.5 km to the east of the transmitter mooring, and was equipped with a VR2AR (RMR_126; Innovasea) at 126 m and a second mid-water column VR2W receiver at 65 m (RMR_65; Innovasea). These receivers were within range (<0.5 km) to detect acoustic transmitters on the transmitter mooring in order to compare the detection efficiency of stationary receivers with the glider-mounted VR2C. While different acoustic receivers (VR2W, VR2AR, and VR2C) were utilized for this study, we expected comparable performance between the similar VR2AR and VR2W models. The primary difference between these receiver models is that VR2ARs have added features to enhance recovery and detecting a broader range of transmitters that are not relevant to this study (Vemco, 2016). It was expected, however, that the VR2C would have reduced detection efficiency when within 0.1 km of the transmitter mooring (Oliver *et al.*, 2017), but would be similar otherwise.

During the range test, the glider was programmed to transit between two waypoints (60.6528°N, −146.329°W, and 60.6905°N, −146.2521°W) separated by 6 km, with the transmitter mooring (Figure 1b) at the centre of the transect line. The glider was set to surface at the two waypoints on the outside of the transect line and every 2 h while transiting along the line. While transecting, the glider was set to dive to 125 m and climb to 3 m below the surface, resulting in average horizontal speeds of 1 km per hour. While underwater, the exact position of the glider in terms of latitude and longitude is unknown. Therefore, the glider's position is approximated by linearly interpolating between the GPS fixes collected at the surface, assuming that the glider travelled in a straight line at constant speed while underwater.

Glider transects are separate instances where the glider passed the transmitter mooring within 1 km and made acoustic detections (Figure 1b; Supplementary Table 1). For each transect, the glider transited the area at a range (Figure 2) of distances (0–1 km), depths (0–130 m), and pitches (−33.9–32°) to evaluate the effect of glider flight variables on acoustic detection efficiency. Transects were also performed on multiple days with varying weather conditions (26–31 January, 1–2 February, 30 March, and 20–21 April). Some tran-

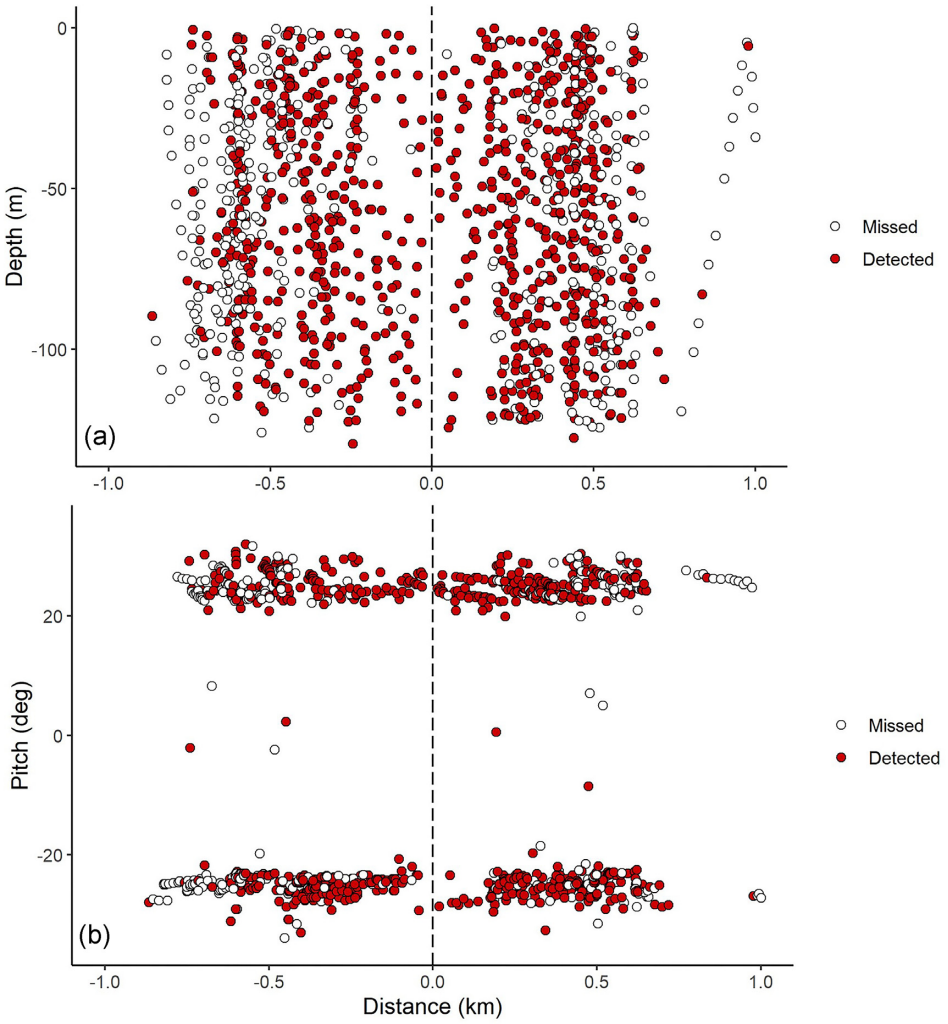

Figure 2. Distance-based dive profile for glider depth (a) and pitch (b) during a range test. The glider conducted 21 transects past a stationary mooring with three acoustic transmitters at varying depths (4, 65, and 119 m). A binary indicator was used to designate whether the onboard VR2C "detected" or "missed" each tag signal transmission at varying distances from the transmitter mooring. Detections were consistently made throughout the depth and distance profile (a), but were restricted to when the pitch of the glider (b) was between 25 ± 3° (climbing) and −25 ± 3° (diving).

sects were removed prior to statistical analysis due to a lack of detections or errors associated with the location of the glider between surface events. A lack of detections occurred for two transects due to the distance of the glider being >1 km from the transmitter mooring for the duration of the transect or because the glider surfaced to transmit data for most of the transect. An additional three transects were removed due to inconsistencies between the interpolated location of the glider between surface events and the recorded location of acoustic detections. This error could be due to stronger currents pushing the glider off of its designated path. In total, 21 transects were included in subsequent analyses.

The transmitter mooring was fit with three acoustic transmitters with a 70–150 s transmission delay. The expected collision rate for three acoustic transmitters with a 70–150 s delay is 10.3 ± 0.1%, which was calculated using the "glatos" package in R (Holbrook *et al.*, 2016). For observed detections, we calculated that 22.8 ± 8.0, 17.5 ± 6.3, and 18.8 ± 6.6% of transmitter pings during 21 glider transects for the surface, mid-water, and bottom transmitters, respectively, were not heard by an acoustic receiver. While our unheard transmission rates were higher than the expected collision rate, they were comparable to previous work with Innovasea acoustic receivers, where a 50–60% detection to transmission ratio is common (Loher *et al.*, 2017). Therefore, statistical analyses only included data for pings that were heard by at least one acoustic receiver.

Detection efficiency (Figure 3) was calculated from the number of transmissions heard by each receiver out of all known transmissions. To normalize detection efficiency for comparison between all four receivers, stationary receiver data were limited to the same timeframes as the 21 glider transects, and the glider-mounted VR2C data were limited to when the glider was within 515 m of the transmitter mooring, the maximum distance between stationary receivers and transmitters (Figure 3c).

GAM modelling

The summed effect of numerous predictor variables on the detection efficiency of stationary and AUV-mounted acoustic receivers for each transmitter (surface, mid-water, and bottom) was evaluated with general additive models (GAM) us-

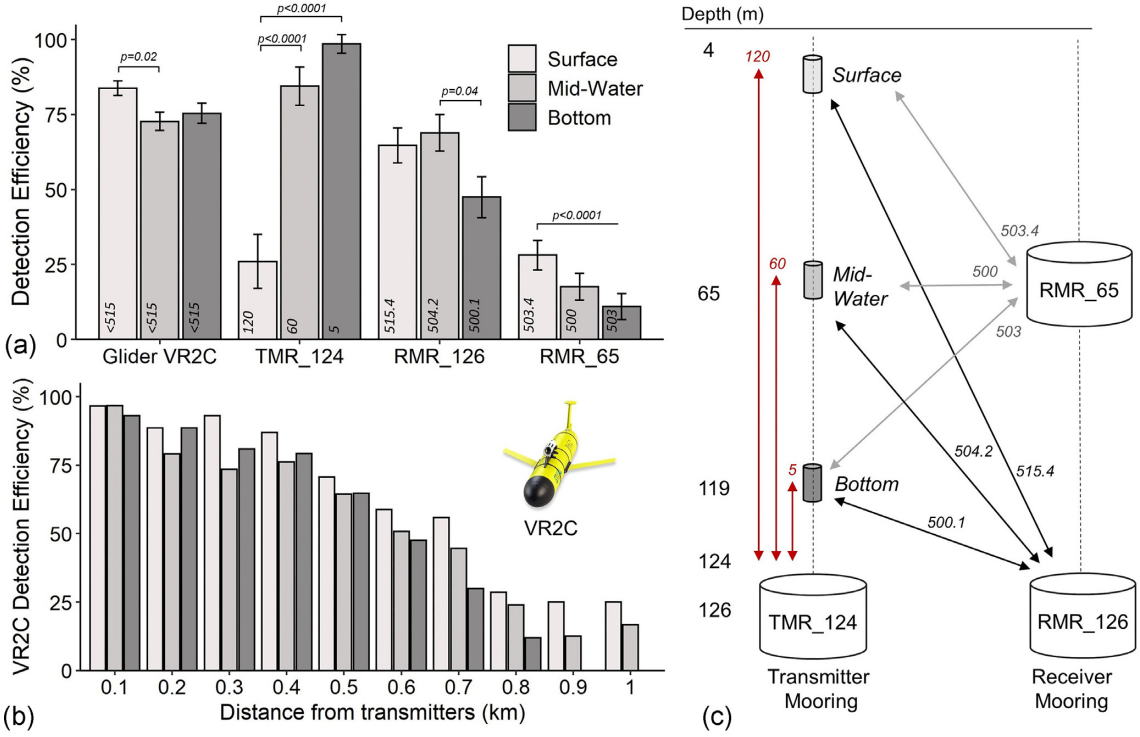

Figure 3. Detection efficiency, the proportion of total transmissions detected (a, b), and mooring designs (c; not drawn to scale). The average detection efficiency (a) of the glider-mounted VR2C, when within 515 m for comparison, and stationary receivers (TMR_124, RMR_126, and RMR_65) for three acoustic transmitters at varying depths (surface; 4 m; mid-water; 65 m; bottom; 119 m). The detection efficiency of the VR2C decreased with distance (b) from the transmitter mooring. The distance (m) between each receiver and transmitter is included at the base of each bar (a) and in the mooring design (c). Significant differences are denoted by a bracket and *p*-value (<0.05).

ing the "mgcv" package in R (Wood, 2015). GAMs were chosen because of their tolerance of nonlinear responses and relaxed distributional assumptions (Zuur *et al.*, 2009). Predictor variables addressed glider flight characteristics including distance, depth, pitch, and orientation. Glider orientation included dive orientation, whether the glider was climbing or diving in the water column, and transmitter orientation, whether the glider-mounted VR2C was pointed at the transmitter mooring or away. Environmental variables were also evaluated and included glider-collected temperature (2.8–11.0°C), salinity (24.6–33.3 PSU), and density (1019.1–1026.4 kg m^{-3}) data, which were used to evaluate ocean stratification and calculated from conductivity and temperature using the seawater equation of state (Fofonoff, 1985). Additional random variables were incorporated, including transect, day, and day/night. Wind and gust speed were collected from NOAA tide station 9454050 (Cordova, AK, USA; 60.5578°N, 145.756°W), while tidal water level and tide direction were obtained from the National Data Buoy Center (Station 46060—West Orca Bay; 60.586°N, 146.787°W). Ambient noise (mV) was collected from TMR_124 (144.8–292.7 mV range), the VR2AR at the base of the transmitter mooring, and is a metric for background noise in proximity to the receiver. The ambient noise metric is constrained to the 69 kHz range of the receiver and is a diagnostic estimate of environmental noise. In previous work, low noise conditions are <300 mV, moderate conditions are 300–650 mV, and high noise conditions are 650–950 mV (Cimino *et al.*, 2018). Ambient noise can impact detections and was included in GAM modelling for both the glider-mounted VR2C and stationary receiver data.

Prior to model fitting, we evaluated the data for gaps in glider coverage (Figure 2) and collinearity of predictor variables. While preliminary models were run with wind speed and/or gust speed, average wind speed was removed from final models due to high collinearity (0.992) with gust speed and minimal contribution to model parsimony. To identify the most parsimonious model, we implemented a stepwise selection of variables (step.Gam in the "gam" package of R; Hastie, 2015) that included combinations of predetermined variables based on previous AUV-based ranged tests (Oliver *et al.*, 2017; Ennasr *et al.*, 2020) and PWS environmental conditions (Vaughan *et al.*, 2001; Campbell, 2018). Predictor variables were excluded from the final model if they did not improve the parsimony of the fitted model.

For all GAMs, cubic regression splines with shrinkage (bs = "cs") were the primary smoothing functions utilized for predictor variables, with estimates using restricted maximum likelihood and a maximum of 12 knots. Shrinkage smoothers were incorporated because they penalize non-significant smoothers, or predictor variables, out of the model (Zuur *et al.*, 2009; Marra and Wood, 2011), and prevent overfitting of the data (Wood, 2000; Wood and Augustin, 2002). Random variables were also incorporated into models (bs = "re"), including transect, day, and day/night. The significance of each smoother was determined by the estimated *p*-value ($p < 0.05$) testing the null hypothesis that the smoothing term is zero and the estimated degrees of freedom. Fitted models were compared using the Akaike information criterion to identify the most parsimonious model for evaluating the partial effect of our predictors on the detection efficiency of all

three acoustic transmitters (surface, mid-water, and bottom). The final check for model fit utilized the gam.check function in "mgcv" as described in Wood (2015) to evaluate the number of knots used for each smoother and determine if patterns were missed in the data and if the distribution of the residuals was non-random.

Because the stationary receivers were continuously detecting transmissions from acoustic transmitters at a range of 0.5 km (Figure 1b), detections were consolidated into a per-hour rate and limited to hours that the AUV came within 1 km of the transmitter mooring. GAM models evaluated the additive effect of predictor variables on the detection rates of the surface, mid-water, and bottom transmitters using a gaussian distribution and an identity link function. The most parsimonious model explained 60.6, 61.5, and 73.3% of the null deviance for the surface, mid-water, and bottom transmitters, respectively, and had the following formula:

$$\begin{aligned} VR2AR/VR2W\ hourly\ detection\ rate\ \sim\ & receiver \\ & + s\left(noise,\ by\ =\ receiver\right) \\ & + s\left(gust\ speed,\ by\ =\ receiver\right) \\ & + s\left(water\ level,\ by\ =\ receiver\right) + tide\ direction \\ & + s\left(day\right) + s\left(day:night\right). \end{aligned}$$

For the AUV-mounted receiver, a binary indicator was used to represent detection (1) or non-detection (0) for every known transmission from each acoustic transmitter (surface, mid-water, and near-bottom). At each transmission, we interpolated glider variables for distance from the transmitter mooring, depth, dive orientation (diving or climbing), mooring orientation (pointing towards mooring, pointing away from mooring), pitch, heading, and environmental variables (temperature, salinity, density, wind speed, gust speed, tidal water level, tide direction, and ambient noise). Random effects were also included (transect, day, and day/night). Data were included from 21 transects (Supplementary Table 1) performed by the AUV between 26 January and 21 April, for a total of 25 h spent transecting. The average time of each transect was 1.2 ± 0.3 h. The most parsimonious model explained 21.5, 17.5, and 28.7% of the null deviance for the surface, mid-water, and bottom transmitters, respectively, and had the following formula:

$$\begin{aligned} VR2C\ detection\ \sim\ & s\left(glider\ distance\right) \\ & + s\left(glider\ depth,\ by\ =\ dive\ orientation\right) \\ & + s\left(glider\ pitch,\ by\ =\ mooring\ orientation\right) \\ & + dive\ orientation + mooring\ orientation \\ & + s\left(gust\ speed\right) + s\left(water\ level\right) \\ & + tide\ direction + s\left(Transect\right). \end{aligned}$$

Herring transects

Throughout all three glider deployments, we monitored data transmissions from the glider as it transited southeastern PWS, an area of ~630 km^2, for detections of herring fit with acoustic transmitters (Model V9-2x; power output 145 dB; battery life 832-d; 70–150 s delay; Innovasea) in April 2019 and 2020 (see Eiler and Bishop, 2016 for acoustic tagging methodology). Herring spawn activity in southeast PWS occurs from late March to early May (McGowan *et al.*, 2021) and is typically concentrated near the mouth of Port Gravina. Based on previous detections recorded using stationary arrays on the southeast PWS spawning grounds (Bishop and Bernard, 2021; M. A. Bishop, unpublished data), we anticipated that acoustically tagged herring would be in the study area during glider deployments between late January and early May. We did not, however, have recent stationary acoustic telemetry data at the time of glider deployment to confirm the presence of tagged herring within PWS.

During each surfacing event, the glider transmitted near real-time detection data that allowed us to implement adaptive sampling strategies, altering the glider path based on detections to revisit areas where herring transmitters were detected. In the absence of herring detections, the glider path was designed to provide optimum coverage of this area, with the most concentrated searches occurring in proximity to coastlines where herring are more likely to be detected (Bishop and Eiler, 2018). We monitored the VR2C data uploads for herring detections daily. When a herring transmitter was detected, the glider path was modified to return to within 1 km of the original location of detection. Re-transiting areas with herring detections allowed for distinguishing transmitters that were shed, ejected from the peritoneal cavity after tagging or the result of a mortality, and were presumed to be stationary on the sea bottom. If herring transmitters were not re-detected during a subsequent transect, herring were designated as alive and having moved away from the area. A herring movement was only designated if a herring transmitter was re-detected in a separate location >1 km from the original detection site.

Results

Range test

Overall, the glider-mounted VR2C detected 65.7% of all acoustic transmissions that occurred during transects when within 1 km of the transmitter mooring. When the glider-mounted VR2C was within a 515 m range, the maximum distance between stationary receivers and transmitters, it had slightly higher detection efficiency for the surface transmitter (83.8%, $p = 0.02$) than the mid-water (72.7%) and bottom transmitters (75.5%; Figure 3a). By comparison, the stationary receivers (TMR_124, RMR_126, and RMR_65) had variable detection efficiency for transmitters that was unexplained by distance alone. The detection efficiency of TMR_124 was 98.5% for the bottom transmitter (5 m above) in comparison to 26% for the surface transmitter (120 m above), despite the distance between the receiver and surface transmitter being within range (<0.5 km) to expect high detectability based on previous range tests for the OTN (Eiler and Bishop, 2016). By contrast, RMR_126 detected 64.7% of surface transmitter pings and had the highest detection efficiency for the mid-water transmitter (68.9%, 504.2 m) and the lowest for the bottom transmitter (47.5%, 500.1 m). The mid-water column receiver, RMR_65, had the lowest overall detection efficiency for all three transmitters, detecting 28 and 11% of transmissions from the surface and bottom transmitters, respectively.

While the average detection efficiency of the glider-mounted VR2C was consistently >70% for all three transmitters, the detectability of the bottom transmitter was the most affected

by distance (Figure 3b). The detection efficiency of the glider-mounted VR2C for the surface and mid-water transmitters remained >50% up to 0.7 and 0.6 km from the transmitter mooring, respectively. For the bottom transmitter, detection efficiency declined at a higher rate than at the surface ($p = 0.03$; *t*-test) and mid-water transmitters ($p = 0.03$), falling <50% between 0.5 and 0.6 km, with no detections once the glider was greater than 0.9 km away. A detection efficiency >75% occurred for all three transmitters when the glider was 0.4–0.5 km away from the transmitter mooring. The closest and farthest detections occurred when the glider was 0.012 and 1.46 km from the transmitter mooring, respectively.

The GAM models for the glider-mounted VR2C identified several predictor variables that differentially affected the detectability of transmitters at varying depths (Figure 4). Distance from the transmitter mooring was the most important variable affecting acoustic detections for all three transmitters (Figure 4a) and was unaffected by the orientation of the glider (pointed towards or away from the transmitter mooring, ascending or descending in the water column, excluded from the model). The model response function for the bottom transmitter corroborated the detection efficiency results (Figure 3b) in that detection probability decreased at a higher rate than for the surface and mid-water transmitters. The model response for all three transmitters indicates that distance reduces the response below the average value (the 0-line) at ~0.5 km.

Glider depth affected acoustic detections at the surface and mid-water transmitters and varied by whether the glider was diving or surfacing (Figure 4b and c), but not by mooring orientation (the glider pointed towards or away from the transmitter mooring, which was excluded from the model). During diving, the glider had the highest detection efficiency for the surface transmitter at ~75 m depth (Figure 4b), with decreasing acoustic detections as depth increased thereafter. Conversely, when surfacing, the glider had higher detection efficiency at depth (~125 m), with acoustic detections being the lowest when closer to the surface (Figure 4c), and presumably closer to the surface transmitter. The detection of the mid-water transmitter was consistent across depths when the glider was diving, but when surfacing, acoustic detections were highest when closer to the surface, decreasing with depth (Figure 4c). Overall, this pattern differed from what was observed for the mid-water column, stationary receiver, RMR_65, which had the lowest detection efficiency (<30%). When the glider-mounted VR2C was at a similar depth (55–75 m) and range (450–550 m) to the RMR_65, the detection probability was 58.8, 63.6, and 68.4% for the surface, mid-water, and bottom transmitters, respectively.

Glider pitch had a minimal effect on the acoustic detections of all three transmitters but varied by mooring orientation, whether the glider was oriented towards or away from the transmitter mooring (Figure 4d and e). Most acoustic detections occurred when the glider was surfacing at a pitch of 25 ± 3° or diving at a pitch of −25 ± 3° (Figure 2b). During transitions between surfacing and diving, the glider only made four detections due to science sampling, including the VR2C, shutting down to prepare data files for transmission upon surfacing. Despite the reduced range of pitch at which the glider-mounted VR2C was able to make acoustic detections, the VR2C detected 20% more transmissions from the mid-water transmitter (Figure 4d, $p = 0.005$) while climbing (positive pitch) than when diving (negative pitch) when oriented towards the transmitter mooring. The VR2C also detected 40% more transmission from the bottom transmitter (Figure 4e, $p = 0.008$) when diving (negative pitch) when oriented away from the transmitter mooring.

The detection efficiency of the glider-mounted VR2C was not affected by ambient ultrasonic noise (excluded from the model), which was recorded by TMR_124. Ambient noise, however, was the most important variable that degraded the detection efficiency of the stationary moorings (Supplementary Figure 1). Ambient noise in excess of 200 mV significantly decreased the detection probability of each stationary acoustic receiver in most cases. Detectability by TMR_124 for the bottom transmitter (positioned 5 m above) was the only instance where detection efficiency was unaffected by ambient noise ($p = 0.5$).

While environmental conditions were expected to affect acoustic detections by the glider-mounted VR2C and stationary moorings, only two variables were included in the final GAM models: gust speed and tidal water level (Figure 5). Additionally, these variables affected the detectability of the stationary receivers more than the glider-mounted VR2C. For gust speed (Figure 5a; 1–13.9 knot range), acoustic detections by the stationary receivers were affected by increasing gust speed. For TMR_124, detectability of the surface and mid-water transmitter decreased ($p < 0.0001$, $p < 0.0001$) with increasing gust speed. The detectability measured by RMR_126, however, was not affected by gust speed ($p = 0.1$, 0.5, and 0.9). For RMR_65, gust speed only reduced the detectability of the mid-water column transmitter ($p = 0.001$). While gust speed affected acoustic detections of stationary receivers, the detectability of the surface, mid-water, and bottom transmitters by the glider-mounted VR2C was unaffected by gust speed ($p = 0.9$, 0.4, and 0.1, respectively).

Water level from tidal fluctuations affected acoustic detections by all four receivers, primarily the surface transmitter (Figure 5b). Higher water levels (>2.5 m) increased the detectability of the surface transmitter for RMR_126 and RMR_65 ($p < 0.0001$; 0.005; Figure 5b), but decreased detectability for TMR_124 ($p = 0.006$). The detectability of the mid-water column transmitter was only affected for RMR_126, increasing after 2.5 m ($p < 0.001$). For the glider-mounted VR2C, the model response for the surface transmitter (Figure 5b) decreased as water level approached 1.5 m and then subsequently increased with increasing water level ($p = 0.006$). Overall, the glider-mounted VR2C and receiver moorings (RMR_126 and RMR_65) had higher acoustic detections at higher water levels, while the transmitter mooring receiver (TMR_124) had fewer (Figure 5b). During glider transects, 20.9 and 18.4% of all acoustic transmissions occurred during water level intervals of 1.8–2.3 and 3.8–4.3 m, respectively, while the remainder were evenly spread (4.6–9.7%) across remaining water levels (−0.6–4.3 m range).

While gust speed and tidal water level were the only environmental variables included in the final GAM models, numerous environmental predictors were evaluated, including ocean stratification. During the range test, the AUV recorded differences in stratification that were not significant predictors (density, temperature, and salinity) identified by the fitted GAM model. In January and February, surface waters were colder (4°C) and fresher (30.25 PSU) than the bottom

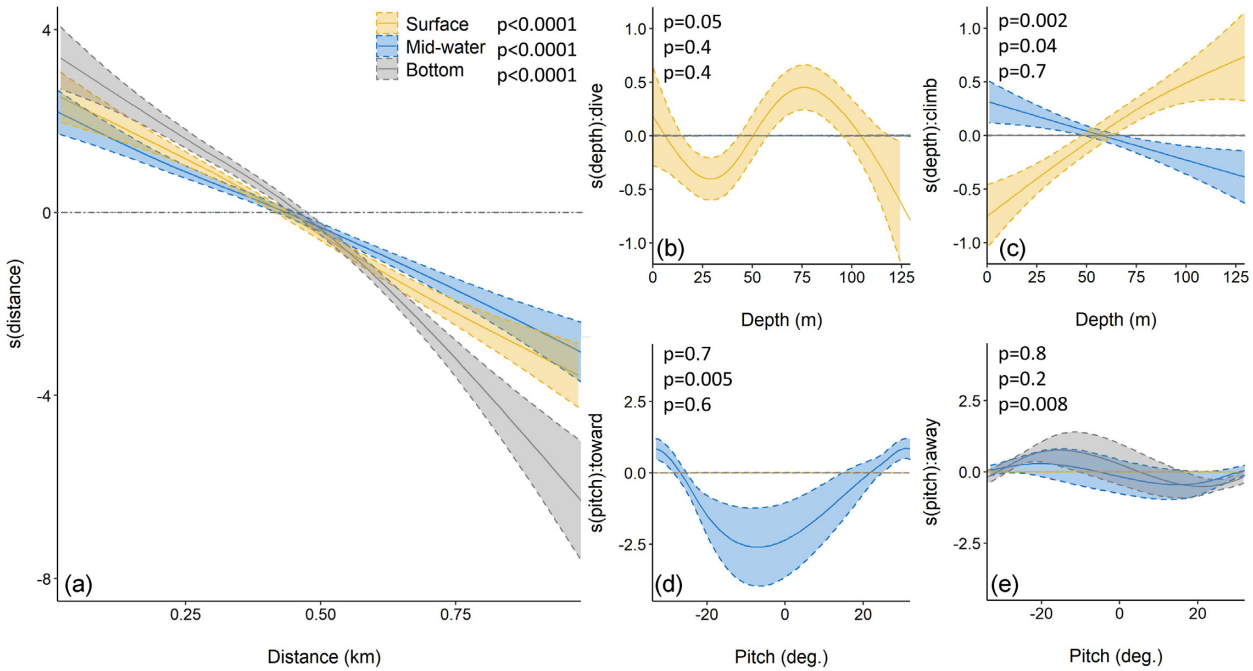

Figure 4. Glider-mounted VR2C model response functions for (a) distance from the transmitter mooring, (b) depth of the glider during dives, (c) depth of the glider during climbs, (d), pitch of the glider when oriented towards the transmitter mooring, and (e), pitch of the glider when oriented away from the transmitter mooring. Dashed lines and shaded regions indicate 95% *CI*. Positive trends indicate that a variable enhances detection efficiency, while negative trends indicate that a variable reduces detection efficiency. *p*-values in the corner of each figure for surface, mid-water, and bottom transmitters, respectively denote significance if <0.05.

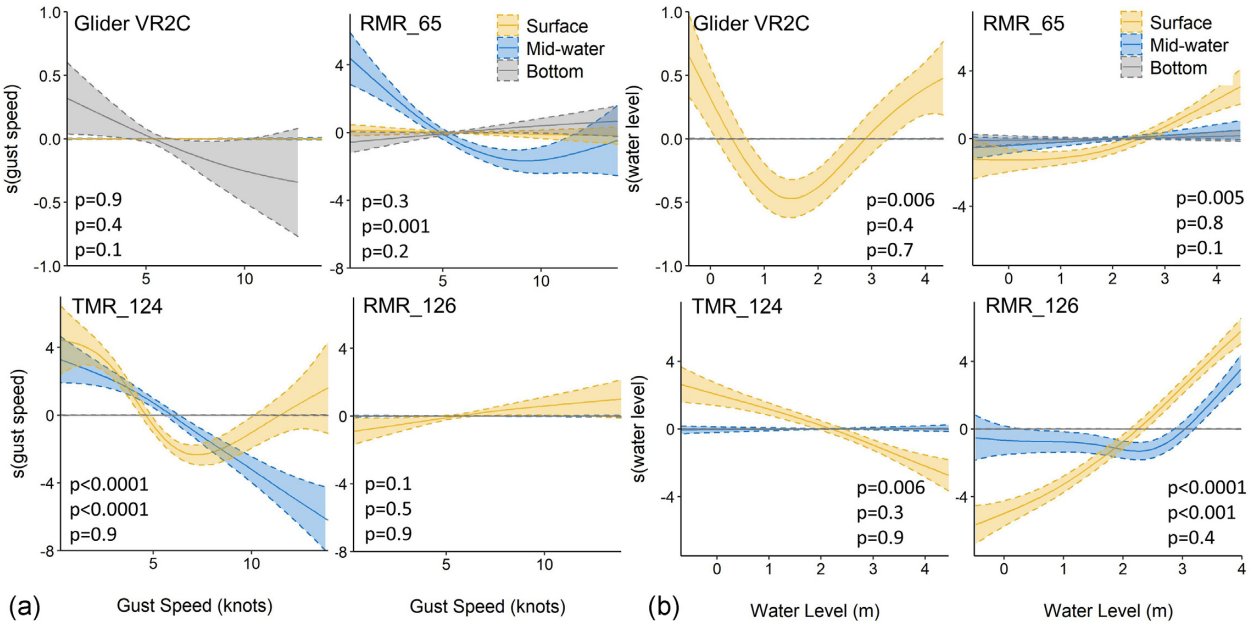

Figure 5. Model response functions for the effect of gust speed (a) and water level (b) on detections by the glider-mounted VR2C and stationary receivers, TMR_124, RMR_126, and RMR_65 (Figure 3c for mooring designs). Dashed lines and shaded regions indicate 95% *CI*. Positive trends indicate that a variable enhances detection efficiency, while negative trends indicate that a variable reduces detection efficiency. *p*-values in the corner of each figure for surface, mid-water, and bottom transmitters, respectively denote significance if <0.05.

(125 m; 6.6°C; 31.75 PSU), with a transition at 35 m depth. In March, the water column was relatively mixed, with a consistent temperature and salinity of 4.5–5°C and 31.5–31.75 PSU, respectively, throughout the water column. In April, a nascent pycnocline was observed at 8 m depth with warmer, fresher water at the surface (6.5°C, 30.75 PSU) in comparison to at depth (125 m, 5°C, 32.0 PSU), but the density difference (~1.3 ± 0.4 kg m^{-3}) was more modest than seen at the seasonal pycnocline of PWS (>6 kg m^{-3}: Campbell, 2018) and does not appear to have impeded detections.

Herring detections

During all three glider deployments, including the range test, the VR2C detected herring transmitters in Port Gravina ($n = 14$), Orca Bay ($n = 12$), Montague Strait ($n = 3$), and the GoA ($n = 1$; Figure 6). In total, the glider detected 30 herring transmitters, including 3 implanted in 2019 and 27 in 2020. Most herring transmitters were detected in proximity to known spawning areas near the mouth of Port Gravina including Knowles Head, Redhead, and Hells Hole, in addition to Orca Bay (Figure 6B). Although the glider was originally directed to pass within 1 km of detected herring during a repeat pass, the results of the range test indicated that 0.5 km (Figure 3b, Figure 4a) is a more suitable range for determining if a herring transmitter is shed or alive. Therefore, of the 30 herring detected, 14 were detected within a 0.5 km range on at least two passes, occurring on separate days, and were therefore designated as shed (Table 2). These shed transmitters were found to be within a range of 1.6–41.8 km from where they were originally released after tagging.

Of the remaining 16 herring transmitters, 8 were designated as alive, and the remaining 8 were designated as undetermined (Table 2). Herring were designated as undetermined when detections occurred during one time period and the area was not re-surveyed within a 0.5 km range. For the herring designated as alive, six were detected during one event at one location, but re-surveying of the area within 0.5 km did not result in a re-detection, indicating that the animal moved away from the area. Lastly, there were two herring detected in two separate locations, demonstrating movement within the inside waters of PWS by 14.8 and 59.5 km (Figure 6; Table 2). The herring that travelled 59.5 km was first detected on 19 April near the mouth of Port Gravina and was re-detected on 5 May 2021, in Montague Strait.

Discussion

Our results support those from previous range tests (Oliver *et al.*, 2017; Ennasr *et al.*, 2020), whereby glider distance, depth, pitch, and orientation are all important variables affecting acoustic detections. While we evaluated a suite of environmental conditions, water level with tidal fluctuations was the only variable that affected acoustic detections by the glider-mounted VR2C. We further demonstrate that the effect of each of these variables differs between transmitters at varying depths (Figure 4). This is an important distinction since range tests do not typically incorporate transmitter depth, even though acoustically tagged animals may be present throughout the water column when within range of an acoustic receiver. Despite this effect, the glider-mounted VR2C had >75% detection efficiency for all three transmitters (surface, mid-water, and bottom) when within 0.5 km. By contrast, stationary receivers positioned 0.5 km from transmitters had lower detection efficiencies (RMR_126; 47–69%, RMR_65; 11–28%) that were more affected by transmitter depth (Figure 3) and environmental conditions (Figure 5).

The effect of transmitter depth on acoustic detections by stationary receivers is typical and important to consider when designing stationary acoustic receiver arrays. Receivers should be positioned to optimally detect acoustic transmissions where they are most likely to occur in the water column (Clements *et al.*, 2005). Typically, acoustic receivers are oriented vertically in the water column and near the ocean bottom to maximize horizontal range and detect transmissions near the sea surface. Conversely, if targeting benthic acoustically tagged animals, the receiver should be positioned upside down near the surface (Clements *et al.*, 2005; Vemco, 2016). In this study, RMR_65 was positioned at mid-depth (~65 m) and experienced the lowest detection efficiency (10–28%) for all three acoustic transmitters (Figure 3a). When the glider-mounted VR2C was at a similar depth (55–75 m) and range (450–550 m) to the RMR_65, the detection probability was >58%. The stationary position of RMR_65, at the same depth as the mid-water transmitter and 60 m above the bottom transmitter, did not provide high detection efficiency due to the hydrophone receiver being oriented towards the surface. However, it is evident that the forward position and mobility of the VR2C on the nose of the glider provided a better 3-D detection range around the VR2C to effectively detect all three transmitters.

Receiver positioning also explains the differences in detection efficiency (Figure 3a) observed between the bottom receivers, TMR_124 and RMR_126, of the transmitter and receiver mooring, respectively. Non-uniform detection areas, often described as the "doughnut effect", can degrade detection efficiency when acoustic transmissions occur within close range (<0.1 km) of the receiver (Kessel *et al.*, 2015; Oliver *et al.*, 2017). This is caused by close proximity detection interference (CPDI), where high-power transmissions encounter reflective barriers, such as the water surface, stratification in the water column, or substrate, causing echoes that interfere with receiver detection (Kessel *et al.*, 2015). This may have contributed to the unexpectedly low detection efficiency of TMR_124 for the surface transmitter, just 120 m above. However, previous range tests using VR2ARs have not demonstrated evidence of CPDI for transmitters with similar power outputs to those used for this study (146 dB; Reubens *et al.*, 2019; Brownscombe *et al.*, 2020). The detection efficiency of TMR_124 for the surface transmitter was, however, the only model response affected by gust speed (Figure 5a), tidal water level (Figure 5b), and ambient ultrasonic noise (Supplementary Figure 1). Therefore, the proximity of the surface transmitter to the sea surface and its susceptibility to environmental conditions, in combination with a non-uniform detection area, may be the cause of poor detection efficiency in this case.

The positional variability of the glider-mounted VR2C during each transect improved its ability to effectively detect transmitters at varying depths in comparison to the stationary receivers (Figure 3a). During each transect, the glider-mounted VR2C continuously changed its distance, depth, and orientation in relation to the transmitter mooring. Unlike the mid-water column receiver (RMR_65), the glider-mounted VR2C had a high probability of making acoustic detections (58.8–68.4%) when at mid-depth (Figure 4b). However, detection efficiency did vary by depth and depend on whether the glider was climbing towards the surface or diving towards the bottom (Figure 4b and c). Even when the hydrophone, which was oriented towards the nose of the glider, was pointed down, it effectively detected the surface transmitter at mid-water depths (Figure 4b). When the glider was climbing, detectability of the surface transmitter decreased as the glider approached the surface (Figure 4c). This may be due to the glider transitioning into surface mode, at which time the VR2C powers down, or the higher susceptibility of VR2Cs to the "doughnut effect" than VR2W and VR2AR models (Oliver *et al.*, 2017). However, there was no evidence of CPDI in our VR2C

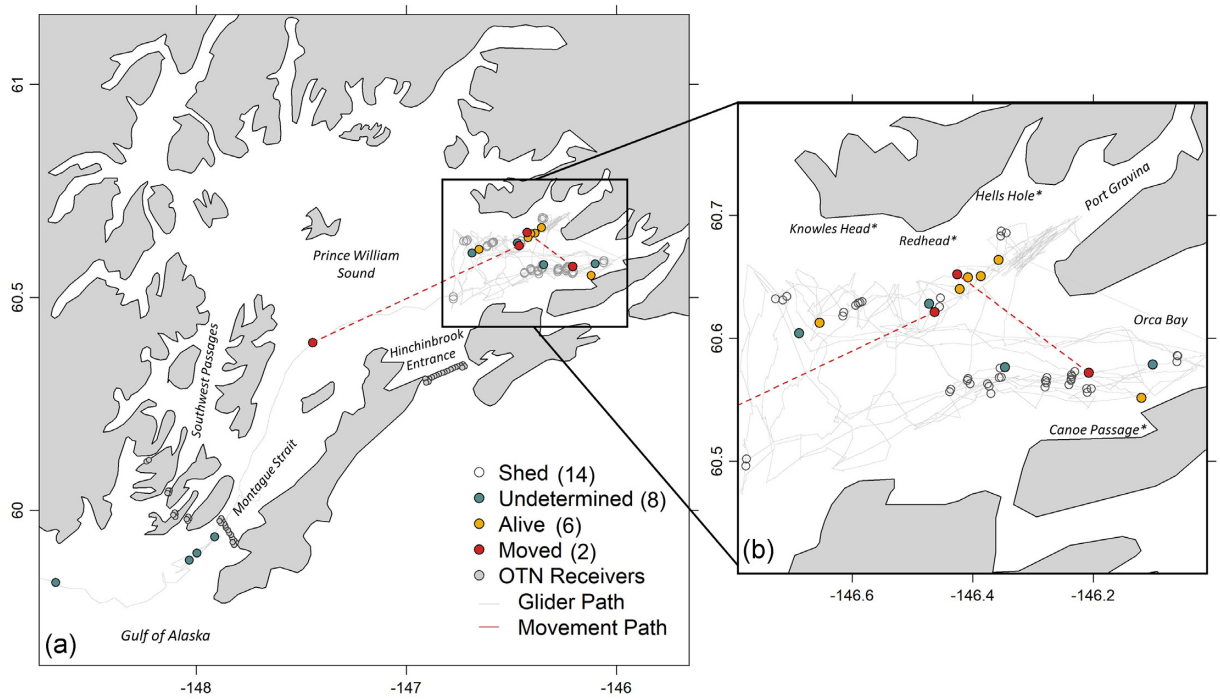

Figure 6. The glider path and acoustic herring transmitters were detected within the entire study area (a) and herring search area (b) near known spawning areas (∗). The glider-mounted VR2C detected a total of 30 herring transmitters implanted into herring in 2019 ($n = 3$) and 2020 ($n = 27$). Transmitters re-detected in the same location were deemed "shed". If the area was not re-surveyed, transmitters were designated as "undetermined". Transmitters detected a single time are deemed "alive" if re-surveying of the area (<0.5 km) does not result in re-detection. Two herring moved between Port Gravina and Orca Bay (15.4 km) and between Port Gravina and Montague Strait (59.5 km). The locations of the OTN receivers at the entrances to PWS are included for reference.

detections (Figure 3b), and the lower power outputs utilized here are not as susceptible to CPDI as higher output transmitters (Kessel *et al.*, 2015).

Environmental conditions affected the detection efficiency of the stationary receivers more than the glider-mounted VR2C (Figure 5). It is evident that the detectability of transmitters closer to the sea surface by the stationary receivers was more susceptible to gust speed and water level while the bottom transmitter was unaffected (Figure 5a). This indicates that OTN receivers may be less efficient during high gust speeds at detecting herring when they are congregating near the surface during feeding but not when they are at depth in the winter months (Carlson, 1980). The glider-mounted VR2C, however, was unaffected by gust speed and therefore may be more likely to detect herring, regardless of depth, during high gust speeds. Water level, however, reduced the detectability of the surface transmitter by the VR2C when water level was ∼1.5 m (−1–4.6 range for Port Gravina; Figure 5b). This may be due to higher ambient noise during tidal fluctuations, which would interfere with acoustic detections (Mathies *et al.*, 2014; Huveneers *et al.*, 2016). However, ambient noise, which was only measured by TMR_124, did not significantly affect the detectability of the glider and was therefore not included in the final model. However, ambient noise conditions for the glider-mounted VR2C likely differ from those for the stationary receivers due to its changing position in the water column, which would expose it to noise events not experienced by the stationary acoustic receivers.

Overall, the detection efficiency of the glider-mounted VR2C was more consistent across transmitters with varying depths (Figure 3a) and detected >75% of detections from each transmitter when <0.5 km from the transmitter mooring. This detection efficiency is similar (∼80%; VR2Tx; Innovasea; Ennasr *et al.*, 2020) or higher than that observed for previous range tests (∼50%; VR2C; Innovasea; Oliver *et al.*, 2017). However, our results corroborate that distance is the greatest predictor of acoustic detections and that orientation (pointing towards transmitters or away), pitch, and depth affect the detectability of transmitters (Oliver *et al.*, 2017; Ennasr *et al.*, 2020). The high detection efficiency observed in this study indicated that the glider-mounted VR2C would have a high probability of detecting acoustically tagged herring during transects throughout the herring search area (Figure 1a) if the AUV came within a 0.5 km range.

During adaptive glider transects within the herring search area (Figure 1a), we detected a total of 30 herring transmitters, 14 of which were presumed shed (Figure 6; Table 2). Because herring are sensitive to handling during acoustic tagging (Seitz *et al.*, 2010), we anticipated that a small percentage of herring transmitters would be shed or the result of post-release mortality. It was, therefore, important to conduct repeated transects to determine if a transmitter was still in a live herring or lying on the ocean bottom. This study was the first demonstration in PWS that shed transmitters could be detected repeatedly within the same area (<1 km). Because these shed transmitters were within close proximity to their original release sites (1.6–41.8 km), we expect that many of these transmitters were shed shortly after tagging. While all three herring transmitters implanted in 2019 were sheds and nearing the end of their battery life at the time of this study, shed transmitters made up 5.9% of the herring tagged in 2020 ($n = 185$). This is comparable to previous work demonstrating that shed and

Table 2. Each herring transmitter detected by the glider-mounted VR2C was designated as "shed", "undetermined", "alive", or "moved" based on whether the area was re-surveyed (Y/N) and whether the transmitter was re-detected.

Designation	Transmitter ID	Area re-surveyed (Y/N)	Detection events
Shed	22 127	Y	6
Shed	22 136	Y	3
Shed	22 140	Y	2
Shed	22 211	Y	3
Shed	56 794	Y	3
Shed	56 807	Y	3
Shed	56 810	Y	3
Shed	56 837	Y	3
Shed	56 864	Y	2
Shed	56 869	Y	3
Shed	56 877	Y	2
Shed	56 878	Y	5
Shed	56 880	Y	4
Shed	56 894	Y	2
Undetermined	22 171	N	1
Undetermined	27 463	N	1
Undetermined	56 865	N	1
Undetermined	56 892	N	1
Undetermined	22 187	N	1
Undetermined	56 868	N	1
Undetermined	56 804	N	1
Undetermined	56 853	N	1
Alive	22 201	Y	1
Alive	56 780	Y	1
Alive	56 782	Y	1
Alive	56 799	Y	1
Alive	56 823	Y	1
Alive	56 848	Y	1
Moved	22 214	Y	2
Moved	56 816	Y	2

Detection events are separate instances (>1 d apart) when the glider detected a transmitter.

mortality rates of herring after transmitter implantation are ~4% each (Seitz *et al.*, 2010).

Of the eight herring designated as undetermined (Figure 6), three were detected in the southern Montague Strait and one in the GoA. Each of these transmitters was only detected once as the glider was unable to re-transit the area due to strong currents toward the GoA. The most recent OTN detections for these herring occurred at the Montague Strait OTN array (Figure 6a for reference), with three occurring 1–4 d prior to detection by the glider-mounted VR2C. These observations suggest that these herring were alive and moving during the time of this study. Importantly, these herring transmitters were the first to be detected south of OTN arrays (Figure 6a for reference) or in the GoA. Based on the timing (post-spawn) and location of detection, we anticipate that these herring were migrating to the GoA for summer foraging.

In total, six herring were designated as alive, while an additional two were detected moving within PWS. In addition, the four undetermined herring detected in Montague Strait and the GoA, and recently detected by OTN receivers, are also likely to be alive. Therefore, 12 of the 30 herring transmitters detected were alive and moving during the time of this study. Of the six herring originally designated as alive, each was detected in close proximity to spawning grounds (Figure 6b) during the 28 March–29 April spawning event (Alaska Department of Fish and Game, unpublished data) in southeast PWS.

We detected two herring movements, demonstrating that the glider-mounted VR2C can re-detect herring within a large herring search area (630 km^2) and relatively short deployment time (86-d). While one herring was detected moving 14.8 km within southeast PWS (Figure 6b), the other herring moved 59.5 km from the spawning grounds to Montague Strait (Figure 6a). The herring detected in Port Gravina and subsequently northern Montague Strait was likely present for spawning during initial detection and then migrating through Montague Strait to exit PWS to the GoA for summer foraging. In addition, this herring was detected on the western side of Montague Strait, suggesting that herring may not be using the more protected bays and coastline habitat on the eastern side of Montague Strait for migration (Figure 6a). In addition, this male herring was the 5th longest (230 mm) and 11th heaviest (146 g) herring tagged with a V9 transmitter ($n = 185$) in 2020. This aligns with OTN acoustic telemetry data, which shows that herring primarily leave PWS through Hinchinbrook Entrance (Figure 6a for reference) after spawning, but that a smaller proportion of larger, older individuals will utilize Montague Strait (Bishop and Bernard, 2021). While this evidence is anecdotal, the ability of the glider to detect any individuals of an original sample size of 185 in a 630 km^2 area without recent release or location data provides strong support for the use of glider-mounted acoustic receivers as supplements to acoustic receiver arrays like the OTN.

Our results demonstrate that glider-mounted acoustic receivers provide consistent detection efficiency of acoustic transmitters at varying depths i.e. >75% when within 0.5 km. In relatively large areas like PWS, the glider was able to detect 14.6% of Pacific herring acoustically tagged with V9 transmitters in 2020, a year prior to this study. While a proportion of these transmitters were shed, the glider was able to discern transmitters from alive fish and detected two herring movements within PWS. Due to the logistics of remotely operating a glider, we were unable to focus our search in near-shore areas where herring are most likely to be detected (Bishop and Eiler, 2018). This is one shortcoming of using a glider-mounted acoustic receiver. However, the glider provided new detections for this study area by detecting shed transmitters near post-tagging release sites and herring transmitters south of the Montague Strait OTN array and in the GoA (Figure 6a). We strongly support the addition of glider-mounted acoustic telemetry to the study of herring movement in PWS and for advancing the study of fish movement in areas where geography and oceanographic conditions prevent expansive stationary receiver coverage.

Acknowledgements

The research described in this study was supported by the Alaska Ocean Observing System (Project #H3027), the Ocean Tracking Network, which provided the acoustic telemetry arrays, and the Exxon Valdez Oil Spill Trustee Council that funded the herring tagging efforts and provided acoustic telemetry equipment.

Supplementary data

Supplementary material is available at the *ICESJMS* online version of the manuscript.

Conflict of interest statement

The authors have no conflicts of interest to declare.

Data availability statement

Acoustic detections and oceanographic data are available through the NOAA National Glider Data Access Center (GDAC) by searching for unit_191, the Teledyne glider utilized for this study, or by using the following link. https://marine.rutgers.edu/cool/data/gliders/dac/status/?filter=gliders&value=unit_191

Author contributions statement

Conceptualization, methodology development, and manuscript review were conducted by all authors. Project administration was conducted by Bishop and Statscewich. Bishop, Campbell, Cypher, and Statscewich carried out the research and data collection. Statscewich performed data curation for AOOS. Cypher conducted the formal data analysis, visualization, and writing.

References

Bishop, M. A., and Bernard, J. W. 2021. An empirical Bayesian approach to incorporate directional movement information from a forage fish into the Arnason–Schwarz mark–recapture model. Movement Ecology, 9: 1–13.

Bishop, M. A., and Eiler, J. H. 2018. Migration patterns of post-spawning Pacific herring in a Subarctic sound. Deep Sea Research Part II: Topical Studies in Oceanography, 147: 108–115.

Breece, M. W., Fox, D. A., Dunton, K. J., Frisk, M. G., Jordaan, A., and Oliver, M. J. 2016. Dynamic seascapes predict the marine occurrence of an endangered species: Atlantic Sturgeon *Acipenser oxyrinchus oxyrinchus*. Methods in Ecology and Evolution, 7: 725–733.

Brownscombe, J. W., Griffin, L. P., Chapman, J.M., Morley, D., Acosta, A., Crossin, G. T., Iverson, S. J. *et al.* 2020. A practical method to account for variation in detection range in acoustic telemetry arrays to accurately quantify the spatial ecology of aquatic animals. Methods in Ecology and Evolution, 11: 82–94.

Cagua, E. F., Berumen, M. L., and Tyler, E. H. M. 2013. Topography and biological noise determine acoustic detectability on coral reefs. Coral Reefs, 32: 1123–1134.

Campbell, R. W. 2018. Hydrographic trends in Prince William Sound, Alaska, 1960–2016. Deep Sea Research Part II: Topical Studies in Oceanography, 147: 43–57.

Carlson, H. R. 1980. Seasonal distribution and environment of Pacific herring near Auke Bay, Lynn Canal, southeastern Alaska. Transactions of the American Fisheries Society, 109: 71–78.

Cimino, M., Cassen, M., Merrifield, S., and Terrill, E. 2018. Detection efficiency of acoustic biotelemetry sensors on wave gliders. Animal Biotelemetry, 6: 1–14.

Clements, S., Jepsen, D., Karnowski, M., and Schreck, C. B. 2005. Optimization of an acoustic telemetry array for detecting transmitter-implanted fish. North American Journal of Fisheries Management, 25: 429–436.

Dodson, T., Grothues, T. M., Eiler, J. H., Dobarro, J. A., and Shome, R. 2018. Acoustic-telemetry payload control of an autonomous underwater vehicle for mapping tagged fish. Limnology and Oceanography: Methods, 16: 760–772.

Eiler, J. H., and Bishop, M. A. 2016. Tagging response and postspawning movements of Pacific herring, a small pelagic forage fish sensitive to handling. Transactions of the American Fisheries Society, 145: 427–439.

Eiler, J. H., Grothues, T. M., Dobarro, J. A., and Masuda, M. M. 2013. Comparing autonomous underwater vehicle (AUV) and vessel-based tracking performance for locating acoustically tagged fish. Marine Fisheries Review, 75: 27–42.

Eiler, J. H., Grothues, T. M., Dobarro, J. A., and Shome, R. 2019. Tracking the movements of juvenile *Chinook salmon* using an autonomous underwater vehicle under payload control. Applied Sciences, 9: 2516.

Ennasr, O., Holbrook, C., Hondorp, D. W., Krueger, C. C., Coleman, D., Solanki, P., Thon, J. *et al.* 2020. Characterization of acoustic detection efficiency using a gliding robotic fish as a mobile receiver platform. Animal Biotelemetry, 8: 1–13.

Exxon Valdez Oil Spill Trustee Council. 2014. 2014 Update Injured Resources and Services List. Anchorage, Alaska, AK.

Fofonoff, N. P. 1985. Physical properties of seawater: a new salinity scale and equation of state for seawater. Journal of Geophysical Research, 90: 3332–3342.

Gjelland, K. Ø., and Hedger, R. D. 2013. Environmental influence on transmitter detection probability in biotelemetry: developing a general model of acoustic transmission. Methods in Ecology and Evolution, 4: 665–674.

Grothues, T. M., Dobarro, J., and Eiler, J. 2010. Collecting, interpreting, and merging fish telemetry data from an AUV: remote sensing from an already remote platform. *In* 2010 IEEE/OES Autonomous Underwater Vehicles, pp. 1–9. IEEE, Piscataway, NJ.https://doi.org/10.1109/AUV.2010.5779658

Grothues, T. M., Dobarro, J., Ladd, J., Higgs, A., Niezgoda, G., and Miller, D. 2008. Use of a multi-sensored AUV to telemeter tagged Atlantic sturgeon and map their spawning habitat in the Hudson River, USA. *In* 2008 IEEE/OES Autonomous Underwater Vehicles, pp. 1–7. IEEE, Piscataway, NJ.https://doi.org/10.1109/AUV.2008.5347597

Hastie, T. 2015. Package 'gam'. https://cran.microsoft.com/snapshot/2017-04-22/web/packages/gam/gam.pdf.

Haulsee, D. E., Breece, M. W., Miller, D. C., Wetherbee, B. M., Fox, D. A., and Oliver, M. J. 2015. Habitat selection of a coastal shark species estimated from an autonomous underwater vehicle. Marine Ecology Progress Series, 528: 277–288.

Holbrook, C., Hayden, T., Binder, T., Pye, J., and Nunes, A. 2016. glatos: a package for the great lakes acoustic telemetry observation system. R Package Version 0.2. 3.

How, J. R., and de Lestang, S. 2012. Acoustic tracking: issues affecting design, analysis and interpretation of data from movement studies. Marine and Freshwater Research, 63: 312–324.

Huveneers, C., Simpfendorfer, C. A., Kim, S., Semmens, J. M., Hobday, A. J., Pederson, H., Stieglitz, T. *et al.* 2016. The influence of environmental parameters on the performance and detection range of acoustic receivers. Methods in Ecology and Evolution, 7: 825–835.

Kessel, S. T., Cooke, S. J., Heupel, M. R., Hussey, N. E., Simpfendorfer, C. A., Vagle, S., and Fisk, A. T. 2014. A review of detection range testing in aquatic passive acoustic telemetry studies. Reviews in Fish Biology and Fisheries, 24: 199–218.

Kessel, S. T., Hussey, N. E., Webber, D. M., Gruber, S. H., Young, J. M., Smale, M. J., and Fisk, A. T. 2015. Close proximity detection interference with acoustic telemetry: the importance of considering tag power output in low ambient noise environments. Animal Biotelemetry, 3: 1–14.

Klinard, N. V., Halfyard, E. A., Matley, J. K., Fisk, A. T., and Johnson, T. B. 2019. The influence of dynamic environmental interactions on detection efficiency of acoustic transmitters in a large, deep, freshwater lake. Animal Biotelemetry, 7: 1–17.

Loher, T., Webster, R. A., and Carlile, D. 2017. A test of the detection range of acoustic transmitters and receivers deployed in deep waters of southeast Alaska, USA. Animal Biotelemetry, 5: 1–22.

Marra, G., and Wood, S. N. 2011. Practical variable selection for generalized additive models. Computational Statistics & Data Analysis. 55: 2372–2387.

Mathies, N. H., Ogburn, M. B., McFall, G., and Fangman, S. 2014. Environmental interference factors affecting detection range in acous-

tic telemetry studies using fixed receiver arrays. Marine Ecology Progress Series, 495: 27–38.
McGowan, D. W., Branch, T. A., Haught, S., and Scheuerell, M. D. 2021. Multi-decadal shifts in the distribution and timing of Pacific herring (*Clupea pallasii*) spawning in Prince William Sound. Canadian Journal of Fisheries and Aquatic Sciences, 78: 1611–1627.
Oliver, M. J., Breece, M. W., Fox, D. A., Haulsee, D. E., Kohut, J. T., Manderson, J., and Savoy, T. 2013. Shrinking the haystack: using an AUV in an integrated ocean observatory to map Atlantic Sturgeon in the coastal ocean. Fisheries, 38: 210–216.
Oliver, M. J., Breece, M. W., Haulsee, D. E., Cimino, M. A., Kohut, J., Aragon, D., and Fox, D. A. 2017. Factors affecting detection efficiency of mobile telemetry slocum gliders. Animal Biotelemetry, 5: 1–9.
Reubens, J., Verhelst, P., van der Knaap, I., Deneudt, K., Moens, T., and Hernandez, F. 2019. Environmental factors influence the detection probability in acoustic telemetry in a marine environment: results from a new setup. Hydrobiologia, 845: 81–94.
Schofield, O., Kohut, J., Aragon, D., Creed, L., Graver, J., Haldeman, C., Kerfoot, J. *et al.* 2007. Slocum gliders: robust and ready. Journal of Field Robotics, 24: 473–485.
Seitz, A. C., Norcross, B. L., Payne, J. C., Kagley, A. N., Meloy, B., Gregg, J. L., and Hershberger, P. K. 2010. Feasibility of surgically implanting acoustic tags into Pacific herring. Transactions of the American Fisheries Society, 139: 1288–1291.
Shroyer, S. M., and Logsdon, D. E. 2009. Detection distances of selected radio and acoustic tags in Minnesota lakes and rivers. North American Journal of Fisheries Management, 29: 876–884.
Vaughan, S. L., Mooers, C. N., and Gay, S. M. 2001. Physical variability in Prince William Sound during the SEA study (1994–98). Fisheries Oceanography, 10: 58–80.
Vemco. 2016. VR2AR User Manual. https://www.oceans-research.com/wp-content/uploads/2016/09/vr2ar-manual.pdf.
Webb, D. C., Simonetti, P. J., and Jones, C. P. 2001. SLOCUM: an underwater glider propelled by environmental energy. IEEE Journal of Oceanic Engineering, 26: 447–452.
White„ C. F., Lin„ Y., Clark„ C. M., and Lowe„ C. G. 2016. Human vs robot: Comparing the viability and utility of autonomous underwater vehicles for the acoustic telemetry tracking of marine organisms. Journal of Experimental Marine Biology and Ecology, 62: 413–428.
Wood, S. 2015. Package 'mgcv'. R Package Version, 1: 729.
Wood, S. N. 2000. Modelling and smoothing parameter estimation with multiple quadratic penalties. Journal of the Royal Statistical Society: Series B (Statistical Methodology), 62: 413–428.
Wood, S. N., and Augustin, N. H. 2002. GAMs with integrated model selection using penalized regression splines and applications to environmental modelling. Ecological Modelling, 157: 157–177.
Zemeckis, D. R., Dean, M. J., DeAngelis, A. I., Van Parijs, S. M., Hoffman, W. S., Baumgartner, M. F., Hatch, L. T. *et al.* 2019. Identifying the distribution of Atlantic cod spawning using multiple fixed and glider-mounted acoustic technologies. ICES Journal of Marine Science, 76: 1610–1625.
Zuur, A. F., Ieno, E. N., Walker, N. J., Saveliev, A. A., and Smith, G. M. 2009. Mixed effects modelling for nested data. *In* Mixed Effects Models and Extensions in Ecology with R, pp. 101–142. Springer, New York, NY.

Handling Editor: Samantha Andrzejaczek